# High–altitude wind power generation

Lorenzo Fagiano, *Member, IEEE,* Mario Milanese*, *Senior Member, IEEE,* and Dario Piga, *Member, IEEE*

***Abstract*—The paper presents the innovative technology of high–altitude wind power generation, indicated as Kitenergy, which exploits the automatic flight of tethered airfoils (e.g. power kites) to extract energy from wind blowing between 200 and 800 meters above the ground. The key points of such technology are described and the design of large scale plants is investigated, in order to show that it has the potential to overcome the limits of the actual wind turbines and to provide large quantities of renewable energy, with competitive cost with respect to fossil sources. Such claims are supported by the results obtained so far in the Kitenergy project, undergoing at Politecnico di Torino, Italy, including numerical simulations, prototype experiments and wind data analyses.**

***Index Terms*—Wind energy, wind power generation, high–altitude wind energy**

## I. Introduction

THE problem of sustainable energy generation is one of the most urgent challenges that mankind is facing today. On the one hand, the world energy consumption is projected to grow by 50% from 2005 to 2030, mainly due to the development of non–OECD (Organization for Economic Cooperation and Development) countries (see [1]). On the other hand, the problems related to the actual distribution of energy production among the different sources are evident and documented by many studies. Fossil fuels (i.e. oil, gas and coal) actually cover about 80% of the global primary energy demand (as reported in [1], updated to 2006) and they are supplied by few producer countries, which own limited reservoirs. The cost of energy obtained from fossil sources is continuously increasing due to increasing demand, related to the rapidly growing economies of the highly populated countries. Moreover, the negative effects of energy generation from fossil sources on global warming and climate change, due to excessive carbon dioxide emissions, and the negative impact of fossil energy on the environment are recognized worldwide and lead to additional indirect costs. One of the key points to solve these issues is the use of a suitable combination of alternative renewable energy sources. However, the actual costs related to such sources are not competitive with respect to fossil energy. An accurate and deep analysis of the characteristics of the various alternative energy technologies is outside the scope of this paper, and only some concise considerations are now reported about wind energy, to better motivate the presented research.

Wind power actually supplies about 0.3% of the global energy demand, with an average global growth of the installed capacity of about 27% in 2007 [2]. It is interesting to note that recent studies [3] showed that by exploiting 20% of the global land sites of class 3 or more (i.e. with average wind speed greater than 6.9 m/s at 80 m above the ground), the entire world's energy demand could be supplied. However, such potential can not be harvested with competitive costs by the actual wind technology, based on wind towers, which require heavy foundations and huge blades, with massive investments. A comprehensive overview of the present wind technology is given in [4], where it is also pointed out that no dramatic improvement is expected in this field. Wind turbines can operate at a maximum height of about 150 m, a value hardly improvably, due to structural constraints which have reached their technological limits. The land occupation of the present wind farms is about 6 towers per $km^2$, considering 1.5 MW, 77–m diameter turbines [5], [6]. The corresponding power density of 9 $MW/km^2$ is about 200–300 times lower than that of large thermal plants. Moreover, due to the wind intermittency, a wind farm is able to produce an average power which is a fraction only of its rated power (i.e. the level for which the electrical system has been designed, see [4]), denoted as "capacity factor" (CF). This fraction is typically in the range 0.3–0.45 for "good" sites. All these issues lead to wind energy production costs that are higher than those of fossil sources. Therefore, a quantum leap would be needed in this field to reach competitive costs with respect to those of the actual fossil sources, thus no more requiring incentives for green energy production.

Such a breakthrough in wind energy generation can be realized by capturing high–altitude wind power. The basic idea is to use tethered airfoils (e.g. power kites like the ones used for surfing or sailing), linked to the ground with cables which are employed to control their flight and to convert the aerodynamical forces into mechanical and electrical power, using suitable rotating mechanisms and electric generators kept at ground level. The airfoils are able to exploit wind flows at higher altitudes than those of wind towers (up to 1000 m), where stronger and more constant wind can be found basically everywhere in the world: thus, this technology can be used in a much larger number of locations. The potentials of such technology has been theoretically investigated almost 30 years ago [7], showing that if the airfoils are driven to fly in "crosswind" conditions, the resulting aerodynamical forces can generate surprisingly high power values. However, only in the past few years more intensive studies have been carried out by some research groups ([8]–[9]), to deeply investigate this idea from the theoretical, technological and experimental point of views. In particular, exploiting the recent advances in the

This research was supported in part by Regione Piemonte, Italy, under the Projects "Controllo di aquiloni di potenza per la generazione eolica di energia", "Generazione eolica di alta quota" and "Power Kites for Naval Propulsion" and by Ministero dell'Università e della Ricerca, Italy, under the National Project "Advanced control and identification techniques for innovative applications".

The authors are with the Dipartimento di Automatica e Informatica, Politecnico di Torino, Torino, Italy

* Corresponding author.

e-mail addresses: lorenzo.fagiano@polito.it, dario.piga@polito.it, mario.milanese@polito.it

modeling and control of complex systems, automated control strategies have been developed to drive the airfoil flight in crosswind conditions. Moreover, small–scale prototypes have been realized to experimentally verify the obtained theoretical and numerical results.

This paper describes the advances of the project Kitenergy, undergoing at Politecnico di Torino, Italy, to develop this technology. Moreover, as a new contribution with respect to previous works (see [8]), which were focused on the control design of a single Kitenergy unit, in this paper several generators operating in the same site are considered and their positions and flight parameters are optimized to maximize the generated power per unit area. This way, the potentials of large scale plants, denoted as KE–farms, are investigated and compared with those of the actual wind tower farms. An analysis of wind speed data collected in some locations in Italy and in the Netherlands is also performed, in order to estimate the CF that can be obtained with Kitenergy. Finally, on the basis of these studies, a preliminary analysis of the costs of the electricity generated with a KE–farm is presented.

It has to be noted that the idea of harvesting the energy of wind flows at high elevation above the ground is being investigated also using different concepts, like the flying electric generators (FEG) described in [10], where generators mounted on tethered rotorcrafts at altitudes of the order of 4600 m are considered. Differently from [10], in the Kitenergy technology the airfoils fly at elevations of at most 800–1000 m above the ground and the bulkier mechanical and electrical parts of the generator are kept at ground level.

As regards the environmental and social impact of the Kitenergy technology, it can be noted that since the airfoils fly at an altitude of 800–1000 m, tethered by two cables of relatively small diameter (about 0.04 m each), their visual and acoustic impacts are significantly lower than those of the actual wind turbines. Moreover the airfoils, being about 50 m wide and 14 m long, project little shadow on the ground, since the sun tends to dissolve the shadow of any object placed at a distance from the ground of approximately 100 times its width. Furthermore, the vast majority of the area occupied by a KE–wind farm is available e.g. for agricultural activities, with reduced risks for safety since the airfoils are very light with respect to their size (e.g. a $20\,m^2$ airfoil weighs about 3 kg) and the breaking of a line or of the kite makes the aerodynamic lift force collapse, making it possible to recover the airfoil by winding back one of the two cables. Finally, for what concerns the effects on bird migration, although it is guessed that the impact of Kitenergy technology may be significantly lower than that of the actual wind towers, due to the different structure of the two systems, specific and detailed analyses will have to be conducted.

The paper is organized as follows. In Section II the concepts of Kitenergy technology are briefly described. Section III resumes the mathematical model employed for numerical analyses in the Kitenergy project and the main numerical and experimental results obtained so far, while Section IV presents the performed wind data analysis and the related CF estimates. Sections V and VI describe the optimization of a KE–farm and the cost analysis respectively. Finally, conclusions are drawn in Section VII.

## II. The Kitenergy project

### A. Basic concepts

The key idea of the Kitenergy project is to harvest high–altitude wind energy with the minimal effort in terms of generator structure, cost and land occupation. In the actual wind towers, the outermost 20% of the blade surface contributes for 80% of the generated power. The main reason is that the blade tangential speed (and, consequently, the effective wind speed) is higher in the outer part, and wind power grows with the cube of the effective wind speed. Thus, the tower and the inner part of the blades do not directly contribute to energy generation. Yet, the structure of a wind tower determines most of its cost and imposes a limit to the elevation that can be reached. To understand the concept of Kitenergy, one can imagine to remove all the bulky structure of a wind tower and just keep the outer part of the blades, which becomes a much lighter kite flying fast in crosswind conditions (see Fig. 1), connected to the ground by two cables, realized in composite materials, with a traction resistance 8–10 times higher than that of steel cables of the same weight. The cables are rolled around two

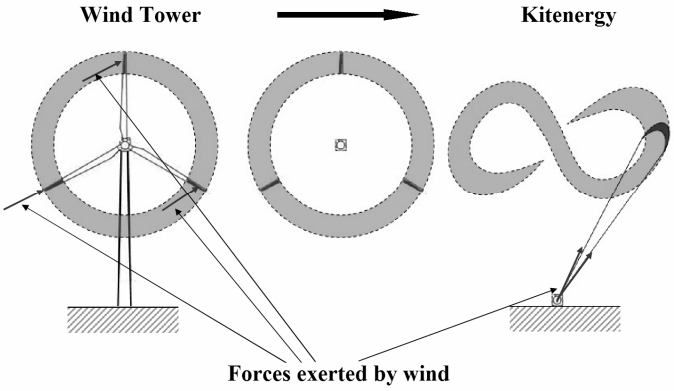


Fig. 1. Basic concept of Kitenergy technology

drums, linked to two electric drives which are able to act either as generators or as motors. An electronic control system can drive the kite flight by differentially pulling the cables (see Fig. 2). The kite flight is tracked and controlled using on–board wireless instrumentation (GPS, magnetic and inertial sensors) as well as ground sensors, to measure the airfoil speed and position, the power output, the cable force and speed and the wind speed and direction. Thus, the rotor and the tower of the present wind technology are replaced in Kitenergy technology by the kite and its cables, realizing a wind generator which is largely lighter and cheaper. For example, in a 2–MW wind turbine, the weight of the rotor and the tower is typically about 250 tons [11]. As reported below, a kite generator of the same rated power can be obtained using a $500–m^2$ kite and cables 1000–m long, with a total weight of about 2 tons only.

The system composed by the electric drives, the drums, and all the hardware needed to control a single kite is denoted as Kite Steering Unit (KSU) and it is the core of the Kitenergy technology. The KSU can be employed in different ways to

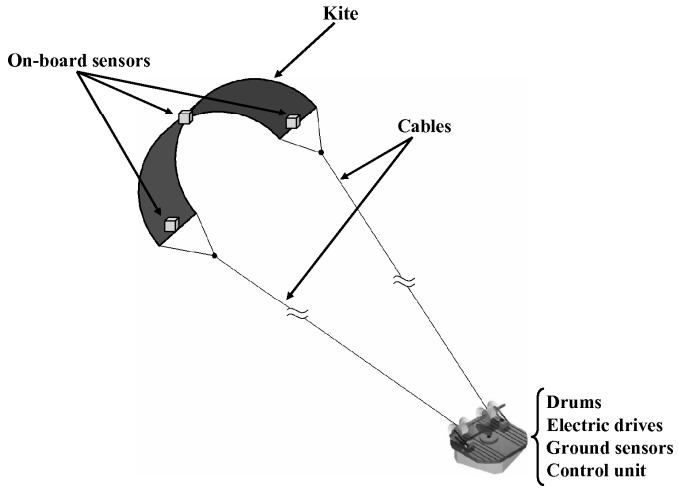


Fig. 2. Scheme of a Kite Steering Unit (KSU)

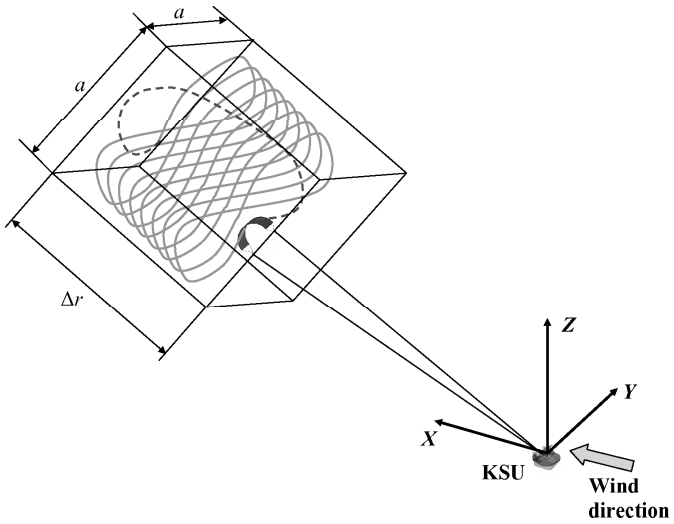


Fig. 3. KE–yoyo configuration cycle: traction (solid) and passive (dashed) phases. The kite is kept inside a polyhedral space region whose dimensions are $(a \times a \times \Delta r)$ meters.

generate energy: two solutions have been investigated so far, namely the KE–yoyo and the KE–carousel configurations (see [8], [12], [13]). In the KE–yoyo generator, wind power is captured by unrolling the kite lines, while in the KE–carousel configuration the KSU is also employed to drag a vehicle, moving along a circular rail path, thus generating energy by means of additional electric generators linked to the wheels. The choice between KE–yoyo and KE–carousel configurations for further developments will be made on the basis of technical and economical considerations, like construction costs, generated power density with respect to land occupation, reliability features, etc. In this paper, the focus is on the analysis of the potential of KE–yoyo generators to operate together in the same site, thus realizing large KE–farms in terms of maximum and average generated power per km$^2$ and energy production costs.

### *B. KE–yoyo energy generation cycle*

In the KE–yoyo configuration, the KSU is fixed with respect to the ground. Energy is obtained by continuously performing a two-phase cycle, depicted in Fig. 3: in the *traction phase* the kite exploits wind power to unroll the lines and the electric drives act as generators, driven by the rotation of the drums. During the traction phase, the kite is maneuvered so to fly fast in crosswind direction, to generate the maximum amount of power. When the maximum line length is reached, the *passive phase* begins and the kite is driven in such a way that its aerodynamic lift force collapses: this way the energy spent to rewind the cables is a fraction (less than 20%) of the amount generated in the traction phase. In the Kitenergy project, numerical and theoretical analyses have been carried out to investigate the potentials of a KE–yoyo unit using the described operating cycle. The results of such studies are resumed in the next Section.

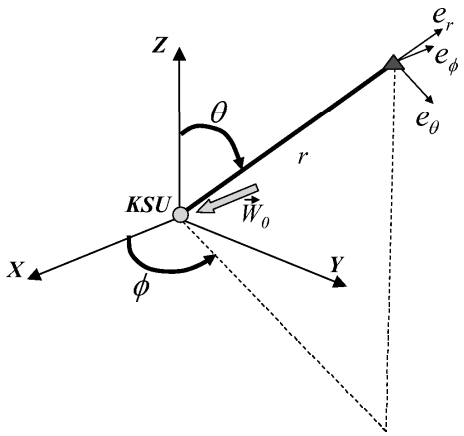


Fig. 4. Model diagram of a KE–yoyo.

## III. KE–YOYO WIND GENERATOR: NUMERICAL AND EXPERIMENTAL RESULTS

### *A. Mathematical model of a KE–yoyo*

In this Section the equations of a mathematical model of a KE–yoyo system are resumed for the sake of completeness (see [12] and [13] for more details).
A Cartesian coordinate system $(X,Y,Z)$ is considered (see. Fig. 4), with $X$ axis aligned with the nominal wind speed vector direction. Wind speed vector is represented as $\vec{W}_l = \vec{W}_0 + \vec{W}_t$, where $\vec{W}_0$ is the nominal wind, supposed to be known and expressed in $(X,Y,Z)$ as:

$$\vec{W}_0 = \begin{pmatrix} W_x(Z) \\ 0 \\ 0 \end{pmatrix} \tag{1}$$

$W_x(Z)$ is a known function which describes the variation of wind speed with respect to the altitude $Z$. In the performed studies, function $W_x(Z)$ corresponds to a wind shear model (see e.g. [3]), which has been identified using the data contained in the database RAOB (RAwinsonde OBservation) of

the National Oceanographic and Atmospheric Administration, see [14]. An example of winter and summer wind shear profiles related to the site of De Bilt in the Netherlands is reported in Fig. 5. The term $\vec{W}_t$ may have components in all

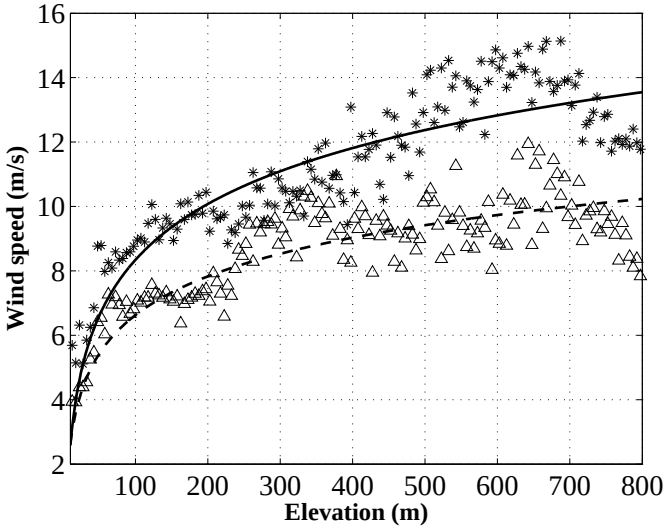


Fig. 5. Wind shear model related to the site of De Bilt, in The Netherlands, for winter months (model: solid line, measured data: asterisks) and for summer months (model: dashed line, measured data: triangles)

directions and is not supposed to be known, accounting for wind unmeasured turbulence.

In system $(X,Y,Z)$, the kite position can be expressed as a function of its distance $r$ from the origin and of the two angles $\theta$ and $\phi$, as depicted in Fig. 4, which also shows the three unit vectors $e_\theta$, $e_\phi$ and $e_r$ of a local coordinate system centered at the kite center of gravity. Unit vectors $(e_\theta, e_\phi, e_r)$ are expressed in the Cartesian system $(X,Y,Z)$ by:

$$\begin{pmatrix} e_\theta & e_\phi & e_r \end{pmatrix} = \begin{pmatrix} \cos(\theta)\cos(\phi) & -\sin(\phi) & \sin(\theta)\cos(\phi) \\ \cos(\theta)\sin(\phi) & \cos(\phi) & \sin(\theta)\sin(\phi) \\ -\sin(\theta) & 0 & \cos(\theta) \end{pmatrix} \tag{2}$$

Applying Newton's laws of motion to the kite in the local coordinate system $(e_\theta, e_\phi, e_r)$, the following dynamic equations are obtained:

$$\begin{aligned} \ddot{\theta} &= \frac{F_\theta}{m\,r} \\ \ddot{\phi} &= \frac{F_\phi}{m\,r\sin\theta} \\ \ddot{r} &= \frac{F_r}{m} \end{aligned} \tag{3}$$

where $m$ is the kite mass. Forces $F_\theta$, $F_\phi$ and $F_r$ include the contributions of gravity force $\vec{F}^{\text{grav}}$ of the kite and the lines, apparent force $\vec{F}^{\text{app}}$, kite aerodynamic force $\vec{F}^{\text{aer}}$, aerodynamic drag force $\vec{F}^{\text{c,aer}}$ of the lines and traction force $F^{\text{c,trc}}$ exerted by the lines on the kite. Their relations, expressed in the local coordinates $(e_\theta, e_\phi, e_r)$ are given by:

$$\begin{aligned} F_\theta &= F_\theta^{\text{grav}} + F_\theta^{\text{app}} + F_\theta^{\text{aer}} + F_\theta^{\text{c,aer}} \\ F_\phi &= F_\phi^{\text{grav}} + F_\phi^{\text{app}} + F_\phi^{\text{aer}} + F_\phi^{\text{c,aer}} \\ F_r &= F_r^{\text{grav}} + F_r^{\text{app}} + F_r^{\text{aer}} + F_r^{\text{c,aer}} - F^{\text{c,trc}} \end{aligned} \tag{4}$$

The following subsections describe how each force contribution is taken into account in the model.

*1) Gravity forces:* the magnitude of the overall gravity force applied to the kite center of gravity is the sum of the kite weight and the contribution given by the weight of the two lines:

$$|\vec{F}^{\text{grav}}| = m\,g + F^{\text{c,grav}} = \left(m + \frac{\rho_l\,\pi\,d_l^2\,r}{4}\right) g \tag{5}$$

where $g$ is the gravity acceleration, $\rho_l$ is the line material density and $d_l$ is the diameter of each line. Vector $\vec{F}^{\text{grav}}$ in the fixed coordinate system $(X,Y,Z)$ is directed along the negative $Z$ direction. Thus, using the rotation matrix (2) the following expression is obtained for the components of $\vec{F}^{\text{grav}}$ in the local coordinates $(e_\theta, e_\phi, e_r)$:

$$\vec{F}^{\text{grav}} = \begin{pmatrix} F_\theta^{\text{grav}} \\ F_\phi^{\text{grav}} \\ F_r^{\text{grav}} \end{pmatrix} = \begin{pmatrix} \left(m + \frac{\rho_l\,\pi\,d_l^2\,r}{4}\right) g\sin(\theta) \\ 0 \\ -\left(m + \frac{\rho_l\,\pi\,d_l^2\,r}{4}\right) g\cos(\theta) \end{pmatrix} \tag{6}$$

*2) Apparent forces:* vector $\vec{F}^{\text{app}}$ accounts for centrifugal inertial forces:

$$\begin{aligned} F_\theta^{\text{app}} &= m(\dot{\phi}^2 r\sin\theta\cos\theta - 2\dot{r}\dot{\theta}) \\ F_\phi^{\text{app}} &= m(-2\dot{r}\dot{\phi}\sin\theta - 2\dot{\phi}\,\dot{\theta}\,r\cos\theta) \\ F_r^{\text{app}} &= m(r\dot{\theta}^2 + r\dot{\phi}^2\sin^2\theta) \end{aligned} \tag{7}$$

*3) Kite aerodynamic forces:* aerodynamic force $\vec{F}^{\text{aer}}$ depends on the effective wind speed $\vec{W}_e$, which in the local system $(e_\theta, e_\phi, e_r)$ is computed as:

$$\vec{W}_e = \vec{W}_l - \vec{W}_a \tag{8}$$

where $\vec{W}_a$ is the kite speed with respect to the ground. Vector $\vec{W}_a$ can be expressed in the local coordinate system $(e_\theta, e_\phi, e_r)$ as:

$$\vec{W}_a = \begin{pmatrix} \dot{\theta}\,r \\ \dot{\phi}\,r\sin\theta \\ \dot{r} \end{pmatrix} \tag{9}$$

Let us consider now the kite wind coordinate system $(\vec{x}_{\text{w}}, \vec{y}_{\text{w}}, \vec{z}_{\text{w}})$ (Fig. 6(a)–(b)), with the origin in the kite center of gravity, $\vec{x}_{\text{w}}$ basis vector aligned with the effective wind speed vector, pointing from the trailing edge to the leading edge of the kite, $\vec{z}_{\text{w}}$ basis vector contained in the kite symmetry plane and pointing from the top surface of the kite to the bottom and wind $\vec{y}_{\text{w}}$ basis vector completing the right handed system. Unit vector $\vec{x}_{\text{w}}$ can be expressed in the local coordinate system $(e_\theta, e_\phi, e_r)$ as:

$$\vec{x}_{\text{w}} = -\frac{\vec{W}_e}{|\vec{W}_e|} \tag{10}$$

According to [15], vector $\vec{y}_{\text{w}}$ can be expressed in the local coordinate system $(e_\theta, e_\phi, e_r)$ as:

$$\vec{y}_{\text{w}} = e_{\text{w}}(-\cos(\psi)\sin(\eta)) + (e_r \times e_{\text{w}})(\cos(\psi)\cos(\eta)) + e_r\sin(\psi) \tag{11}$$

where:

$$\begin{aligned} e_{\text{w}} &= \frac{\vec{W}_e - e_r(e_r\cdot\vec{W}_e)}{|\vec{W}_e - e_r(e_r\cdot\vec{W}_e)|} \\ \eta &\doteq \arcsin\left(\frac{\vec{W}_e\cdot e_r}{|\vec{W}_e - e_r(e_r\cdot\vec{W}_e)|}\tan(\psi)\right) \end{aligned} \tag{12}$$

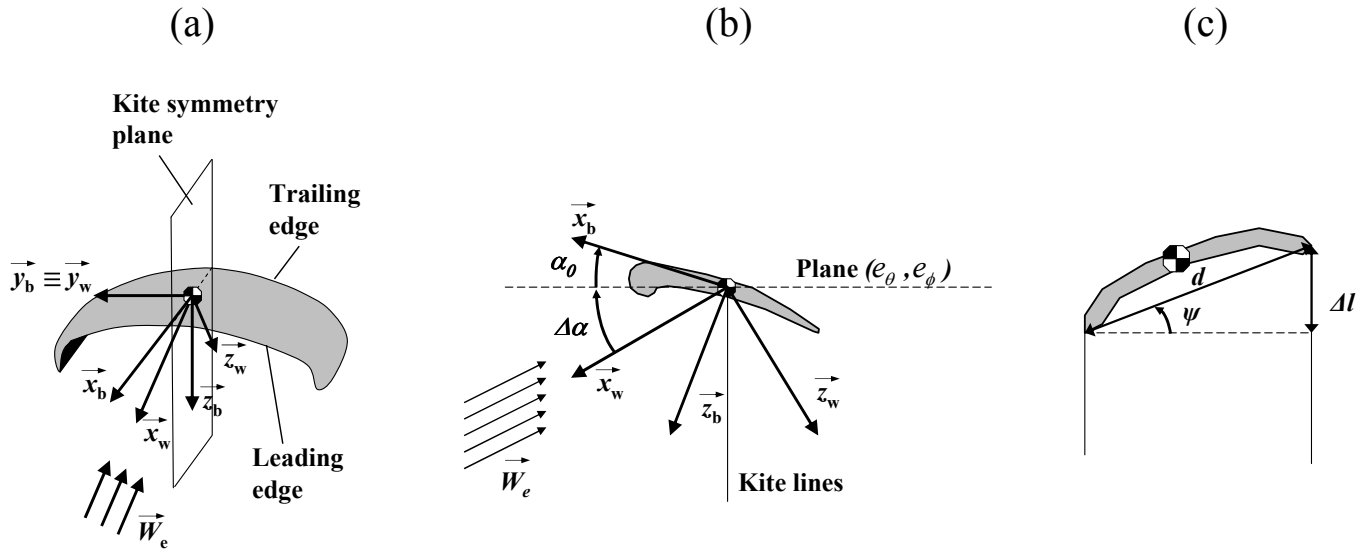


Fig. 6. (a) Scheme of the kite wind coordinate system $(\vec{x}_\mathrm{w},\vec{y}_\mathrm{w},\vec{z}_\mathrm{w})$ and body coordinate system $(\vec{x}_\mathrm{b},\vec{y}_\mathrm{b},\vec{z}_\mathrm{b})$. (b) Wind axes $(\vec{x}_\mathrm{w}, \vec{z}_\mathrm{w})$, body axes $(\vec{x}_\mathrm{b}, \vec{z}_\mathrm{b})$ and angles $\alpha_0$ and $\Delta\alpha$. (c) Command angle $\psi$

Angle $\psi$ is the control input, defined by

$$\psi = \arcsin\left(\frac{\Delta l}{d}\right) \tag{13}$$

with $d$ being the distance between the two lines fixing points at the kite and $\Delta l$ the length difference of the two lines (see Fig. 6(b)). $\Delta l$ is considered positive if, looking the kite from behind, the right line is longer than the left one. Equation (11) has been derived in [15] in order to satisfy the requirements that $\vec{y}_\mathrm{w}$ is perpendicular to $\vec{x}_\mathrm{w}$, that its projection on the unit vector $e_r$ is $\vec{y}_\mathrm{w}\cdot e_r = \sin(\psi)$ and that the kite is always in the same orientation with respect to the lines. Angle $\psi$ influences the kite motion by changing the direction of vector $\vec{F}^\mathrm{aer}$. Finally, the wind unit vector $\vec{z}_\mathrm{w}$ can be computed as:

$$\vec{z}_\mathrm{w} = \vec{x}_\mathrm{w}\times\vec{y}_\mathrm{w} \tag{14}$$

Then, the aerodynamic force $\vec{F}^\mathrm{aer}$ in the local coordinate system $(e_\theta, e_\phi, e_r)$ is given by:

$$\vec{F}^\mathrm{aer} = \begin{pmatrix} F_\theta^\mathrm{aer} \\ F_\phi^\mathrm{aer} \\ F_r^\mathrm{aer} \end{pmatrix} = -\frac{1}{2}C_D A\rho\,|\vec{W}_e|^2\vec{x}_\mathrm{w} - \frac{1}{2}C_L A\rho\,|\vec{W}_e|^2\vec{z}_\mathrm{w} \tag{15}$$

where $\rho$ is the air density, $A$ is the kite characteristic area, $C_L$ and $C_D$ are the kite lift and drag coefficients. As a first approximation, the drag and lift coefficients are nonlinear functions of the kite angle of attack $\alpha$. To define angle $\alpha$, the kite body coordinate system $(\vec{x}_\mathrm{b},\vec{y}_\mathrm{b},\vec{z}_\mathrm{b})$ needs to be introduced (Fig. 6(a)–(b)), centered in the kite center of gravity with unit vector $\vec{x}_\mathrm{b}$ contained in the kite symmetry plane, pointing from the trailing edge to the leading edge of the kite, unit vector $\vec{z}_\mathrm{b}$ perpendicular to the kite surface and pointing down and unit vector $\vec{y}_\mathrm{b}$ completing a right–handed coordinate system. Such a system is fixed with respect to the kite. The attack angle $\alpha$ is then defined as the angle between the wind axis $\vec{x}_\mathrm{w}$ and the body axis $\vec{x}_\mathrm{b}$ (see Fig. 6(a)). Note that in the employed model, it is supposed that the wind axis $\vec{x}_\mathrm{w}$ is always contained in the kite symmetry plane. Moreover, it is considered that by suitably regulating the attack points of the lines to the kite, it is possible to impose a desired *base* angle of attack $\alpha_0$ to the kite: such an angle (depicted in Fig. 6(a)) is defined as the angle between the kite body axis $\vec{x}_\mathrm{b}$ and the plane defined by local vectors $e_\theta$ and $e_\phi$, i.e. the tangent plane to a sphere with radius $r$. Then, the actual kite angle of attack $\alpha$ can be computed as the sum of $\alpha_0$ and the angle $\Delta\alpha$ between the effective wind $\vec{W}_e$ and the plane defined by $(e_\theta, e_\phi)$:

$$\begin{aligned} \alpha &= \alpha_0 + \Delta\alpha \\ \Delta\alpha &= \arcsin\left(\frac{e_r\cdot\vec{W}_e}{|\vec{W}_e|}\right) \end{aligned} \tag{16}$$

Functions $C_L(\alpha)$ and $C_D(\alpha)$ employed in the analyses presented in this paper are reported in Fig. 7(a), while the related aerodynamic efficiency $E(\alpha) = C_L(\alpha)/C_D(\alpha)$ is reported in Fig. 7(b). Such curves refer to a kite with a Clark–Y profile and a curved shape, with effective area equal to 500 m$^2$ and flat aspect ratio (i.e. length of flat wingspan divided by the average kite chord) equal to 4.9 and they have been obtained using CFD analysis with the STAR–CCM+® code (see e.g. [16]). The flat kite wingspan is equal to 56 m, while the center chord is equal to 14.5 m. The related Reynolds number, computed on the basis of the average kite chord (i.e. about 11 m) and considering an effective wind speed of 40 m/s, is about $30\,10^6$.

*4) Line forces:* the lines influence the kite motion through their weight (see Section III-A1), their drag force $\vec{F}^\mathrm{c,aer}$ and the traction force $F^\mathrm{c,trc}$. An estimate of the drag of the lines can be computed as (see [13], [17]):

$$\vec{F}^\mathrm{c,aer} = \begin{pmatrix} F_\theta^\mathrm{c,aer} \\ F_\phi^\mathrm{c,aer} \\ F_r^\mathrm{c,aer} \end{pmatrix} = -\frac{\rho\,C_{D,l}\,r\,d_l\cos(\Delta\alpha)}{8}|\vec{W}_e|^2\vec{x}_\mathrm{w} \tag{17}$$

where $C_{D,l}$ is the line drag coefficient.
The traction force $F^\mathrm{c,trc}$ is always directed along the local unit

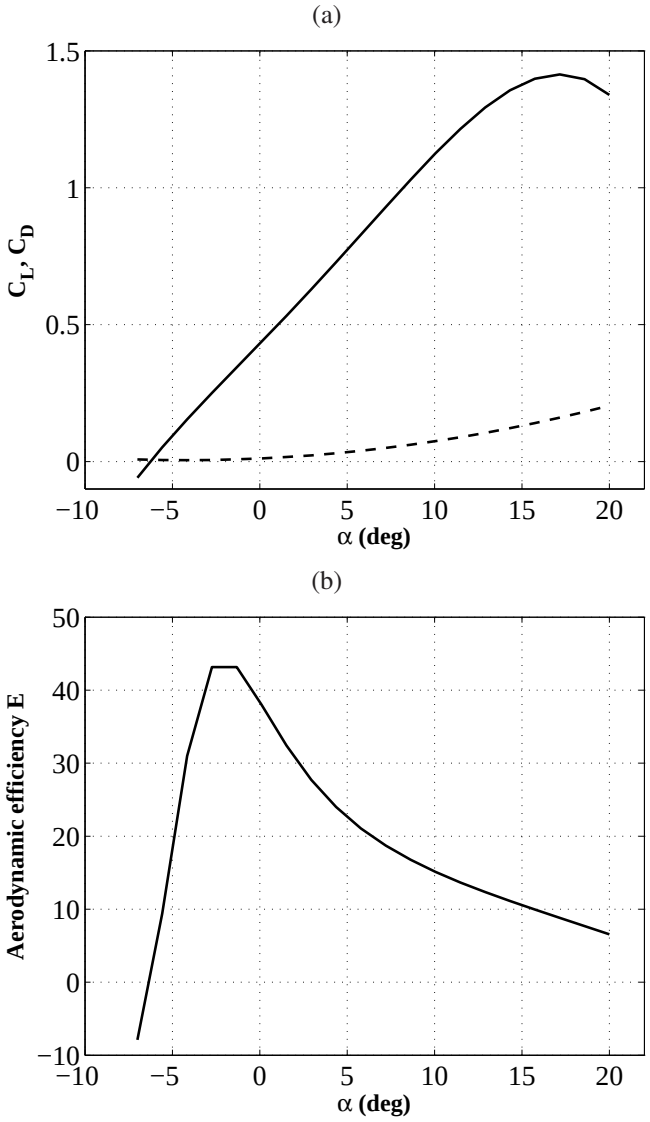


Fig. 7. (a) Kite Lift coefficient $C_L$ (solid) and drag coefficient $C_D$ (dashed) as functions of the attack angle $\alpha$. (b) Aerodynamic efficiency $E$ as function of the attack angle $\alpha$.

vector $e_r$ and can not be negative in equation (4), since the kite can only pull the lines. Moreover, $F^{\text{c,trc}}$ is measured by a force transducer on the KSU and, using a local controller of the electric drives, it is regulated in such a way that $\dot{r}(t) \approx \dot{r}_{\text{ref}}(t)$, where $\dot{r}_{\text{ref}}(t)$ is chosen to achieve a good compromise between high line traction force and high line winding speed. Basically, the stronger the wind, the higher the values of $\dot{r}_{\text{ref}}(t)$ that can be set obtaining high force values. It results that $F^{\text{c,trc}}(t) = F^{\text{c,trc}}(\theta, \phi, r, \dot{\theta}, \dot{\phi}, \dot{r}, \dot{r}_{\text{ref}}, \vec{W}_t)$.

*5) Overall model equations and generated power:* The model equations (3)–(17) give the system dynamics in the form:

$$\dot{x}(t) = f(x(t), u(t), \dot{r}_{\text{ref}}(t), \vec{W}_t(t)) \tag{18}$$

where $x(t) = [\theta(t)\ \phi(t)\ r(t)\ \dot{\theta}(t)\ \dot{\phi}(t)\ \dot{r}(t)]^T$ are the model states and $u(t) = \psi(t)$ is the control input. All the model states are supposed to be measured or estimated, to be used for feedback control. The net electrical power $P$ generated (or spent) by the generator due to line unrolling (or winding back) is given by:

$$P(t) = \eta_{\text{e}} \dot{r}(t) F^{\text{c,trc}}(t) \tag{19}$$

where $\eta_{\text{e}} \in (0,1)$ is a coefficient that takes into account the efficiencies of the mechanical transmission and of the electric drives of the KSU. Note that a static gain (i.e. $\eta_{\text{e}}$) is used to describe such components instead of a dynamical model, since the dynamics of the mechanical transmission and of the electric drives are much faster than those of the kite movement. As anticipated, the model (18) can be used to perform numerical simulations of a KE–yoyo, in order to evaluate its energy generation potentials. The results of such analyses are resumed in Section III-C.

### *B. Simplified theoretical crosswind kite power equations*

The differential equations (18) allow to simulate the operation of a KE–yoyo and to evaluate the capability of controlling the kite flight, maximizing the generated energy while preventing the kite from falling to the ground and the lines from entangling. Moreover, numerical simulations make it possible to evaluate the effects of wind turbulence on the system. However, simulation of the system via numerical integration of (18) takes a relatively large amount of time. Thus, a simplified static theoretical equation, giving the generated power as a function of the wind speed and of the kite position, is useful to perform first–approximation studies of the performance of a KE–yoyo and to optimize its operational parameters. Moreover, such an equation can be also used to optimize the operation of a KE–farm, as it will be shown in Section V. The simplified theoretical equation of crosswind kite power, already derived in the literature (see e.g. [7], [13], [9]), is based on the following hypotheses:

- the airfoil flies in crosswind conditions;
- the inertial and apparent forces are negligible with respect to the aerodynamic forces;
- the kite speed relative to the ground is constant;
- the kite angle of attack is fixed.

Given these assumption, the average mechanical power $\overline{P}_{\text{KE–yoyo}}$ generated by a KE–yoyo unit during a cycle can be computed as:

$$\overline{P}_{\text{KE–yoyo}} = \eta_{\text{e}} \eta_{\text{c}} C \left| W_x(\overline{Z}) \sin(\theta) \cos(\phi) - \dot{r}^{\text{trac}} \right|^2 \dot{r}^{\text{trac}} \tag{20}$$

where

$$\begin{aligned} \overline{Z} &= \cos(\theta)(\overline{r} + \underline{r})/2 \\ C &= \frac{1}{2} \rho A \overline{C}_L E_{\text{eq}}^2 \left(1 + \frac{1}{E_{\text{eq}}^2}\right)^{\frac{3}{2}} \\ E_{\text{eq}} &= \frac{\overline{C}_L}{C_{D,\text{eq}}} \\ C_{D,\text{eq}} &= \overline{C}_D \left(1 + \frac{(2 r d_l) C_{D,l}}{4 A \overline{C}_D}\right) \end{aligned} \tag{21}$$

and $\eta_{\text{c}} \in (0,1)$ is a coefficient accounting for the losses of the energy generation cycle of a KE–yoyo. $\underline{r}$ and $\overline{r}$ are the minimum and maximum values of the cable length during a KE–yoyo cycle (i.e. at the beginning and at the end of each traction phase respectively), while $\overline{C}_L$ and $\overline{C}_D$ are the

aerodynamic coefficients corresponding to the considered fixed angle of attack of the airfoil. Finally, $\dot{r}^{\text{trac}}$ is the line unrolling speed during the traction phase. The traction force generated on the lines can be also computed with a simplified equation as follows:

$$F^{\text{c,trc}} = C\left|W_x(\overline{Z})\sin(\theta)\cos(\phi) - \dot{r}^{\text{trac}}\right|^2 \qquad (22)$$

### C. Numerical analyses

The operational cycle of a KE–yoyo described in Section II-B has been developed and tested through numerical simulations [12], [13], using the model (18) with Matlab® Simulink® and employing advanced control techniques to maximize the net generated energy. In particular, a Nonlinear Model Predictive Control (NMPC, see e.g. [18]) strategy has been employed. Such a control strategy, based on the real–time solution of a constrained optimization problem, allows to maximize the generated energy while explicitly taking into account the state and input constraints, related to actuator limitations and to the need of preventing the airfoil from falling to the ground and the lines from entangling. However, the use of NMPC techniques is limited by the inability of solving the inherent numerical optimization problem at the required sampling time (of the order of 0.2 s): thus, a fast implementation technique of the NMPC law, denoted as FMPC (see [19] and [20]), is used. According to the obtained simulation results, the controller is able to stabilize the system and the flight trajectory is kept inside a space region which is limited by a polyhedron of given dimension $a \times a \times \Delta r$ (see Fig. 3). The value of $a$ depends on the kite size and shape, which influences its minimal turning radius during the flight: a minimal value of $a \simeq 5w_s$ has been assumed, where $w_s$ is the airfoil wingspan. For example, it results that a $500\,\text{m}^2$ kite is able to fly in a zone contained in a polyhedron with $a = 300\,\text{m}$. $\Delta r$ is a design parameter which imposes the maximal range of cable length variation during the KE–yoyo cycle and it can be optimized on the basis of the airfoil and wind characteristics (see Section V and [12], [13]). The control system is able to keep the kite flight inside the polyhedral zone also in the presence of quite strong turbulence (see [12], [13]).

Table I shows the characteristics of the KE–yoyo model employed in the numerical simulations. The aerodynamic characteristics considered for the simulations are those reported in Fig. 7. From such simulations, the power curve of the considered KE–yoyo has been computed (see Fig. 8): such a curve gives the generated power as a function of wind speed and it can be employed to compare the performances of the KE–yoyo with those of a commercial wind turbine with the same rated power (i.e. 2 MW), whose power curve (see e.g. [11]) is reported in Fig. 8 too. In particular, it can be noted that a net power value of 2 MW is obtained by the KE–yoyo with 9–m/s wind speed, while a commercial wind tower can produce only 1 MW in the same conditions. Note that the power curves are saturated at the rated value of 2 MW, corresponding to the maximum that can be obtained with the employed electric equipment. Moreover, for the Kitenergy a cut–out wind speed of 25 m/s has been also considered, as it is done for wind turbines for structural safety reasons, though it is expected that a KE–yoyo could be able to operate at its maximal power with wind speeds up to 40–50 m/s.

TABLE I
KE–YOYO MODEL PARAMETERS EMPLOYED IN THE NUMERICAL SIMULATIONS AND IN EQUATION (20).

| | | |
|---|---|---|
| Kite mass (kg) | $m$ | 300 |
| Characteristic area ($\text{m}^2$) | $A$ | 500 |
| Base angle of attack (°) | $\alpha_0$ | 3.5 |
| Diameter of a single line (m) | $d_l$ | 0.03 |
| Line density ($\text{kg/m}^3$) | $\rho_l$ | 970 |
| Line drag coefficient | $C_{D,l}$ | 1.2 |
| Minimum cable length (m) | $\underline{r}$ | 850 |
| Maximum cable length (m) | $\overline{r}$ | 900 |
| Air density ($\text{kg/m}^3$) | $\rho$ | 1.2 |
| Average kite lift coefficient | $\overline{C}_L$ | 1.2 |
| Average kite drag coefficient | $\overline{C}_D$ | 0.089 |
| KSU efficiency | $\eta_{\text{e}}$ | 0.8 |
| KE–yoyo cycle efficiency | $\eta_{\text{c}}$ | 0.7 |

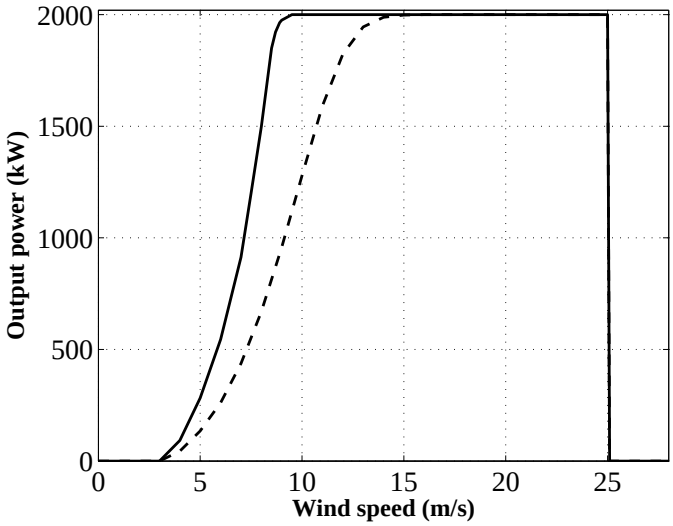


Fig. 8. Comparison between the power curves of a typical wind tower (dashed) and of a KE–yoyo (solid), both with the same rated power of 2 MW.

Numerical simulations have been also employed to investigate the dependance of the mean generated power on the kite area and efficiency, on the average cable length during the cycle and on wind speed. In the performed simulations, if not differently specified, a kite with the characteristics of Table I has been considered. Note that in all the simulations, the cable diameter has been dimensioned in accordance with the traction force exerted by the kite, which vary with the different considered parameter values. To this end, the breaking load characteristics of the polyethylene fiber composing the cables, reported in Fig. 9, has been employed considering a safety coefficient equal to 1.2. The main results of the scalability studies are resumed in Fig. 10–13. Such studies also allowed to assess the good matching between the numerical simulation results and the theoretical values obtained with equation (20) (see Fig. 10–13, solid lines). Basically, the generated power increases linearly with the kite area (Fig. 10) and according to a logistic–type function with the kite aerodynamic efficiency (Fig. 11). As regards the dependence on the average line length, it can be observed (Fig. 12) that there is an optimal point (which

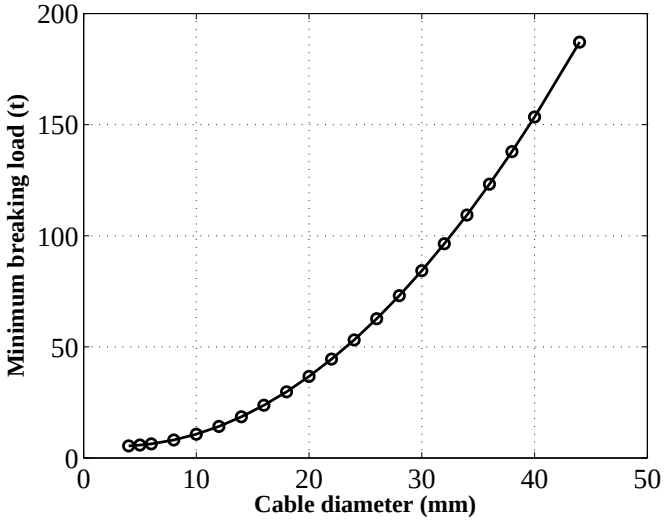


Fig. 9. Breaking load characteristic as a function of diameter of the cable.

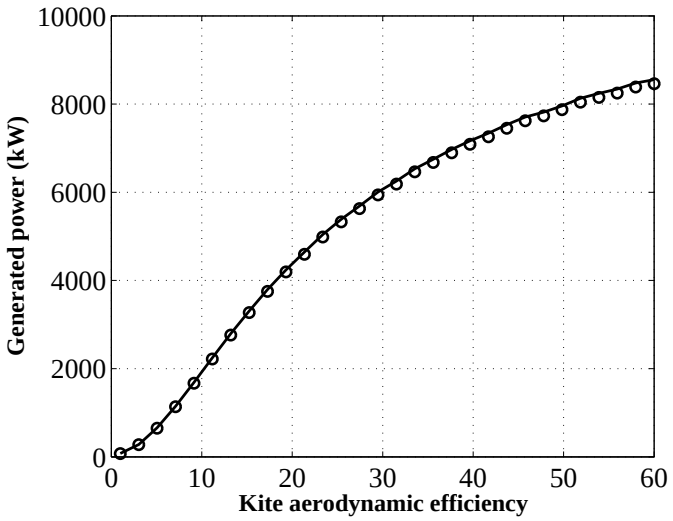


Fig. 11. Obtained net power as a function of kite aerodynamic efficiency: numerical simulation (circles) and theoretical equation (solid line) results.

depends on the wind–elevation characteristic $W_x(Z)$) in which the positive effect of higher wind speed values, obtained with longer cables, is counter–balanced by the negative effect of higher cable weight and drag force. Beyond this point, an increase of cable length leads to lower mean generated power. Finally it can be noted that, as expected from aerodynamic laws, a cubic relationship exists between the generated power

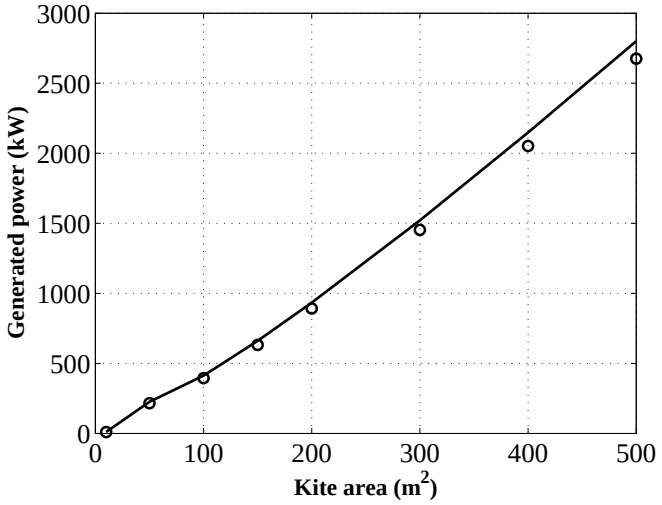


Fig. 10. Obtained net power as a function of kite area: numerical simulation (circles) and theoretical equation (solid line) results.

and the wind speed (Fig. 13). In particular, note that the same 500–m$^2$ kite can be used to obtain either a KE–yoyo with 2–MW rated power, with 9–m/s wind speed, or a KE–yoyo with 5–MW rated power, with about 12–m/s wind speed, without a significant cost increase, except for the electric equipments. Such consideration is useful to perform a preliminary estimate of the energy production potential of a KE–farm and of the related energy cost (see Sections V and VI below).

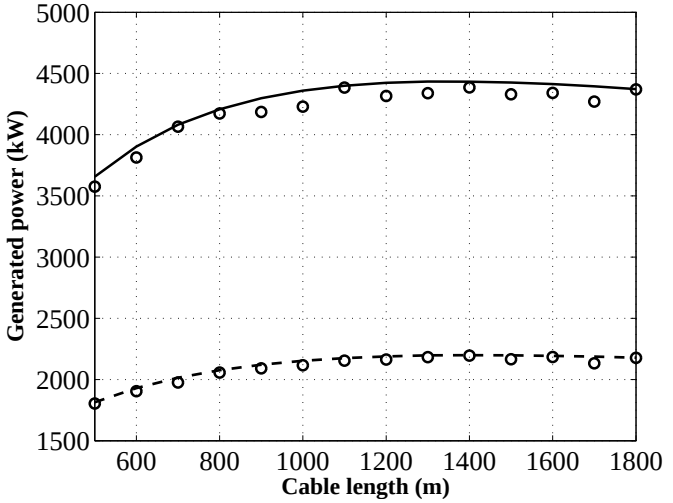


Fig. 12. Obtained net power as a function of cable length for winter (solid) and summer (dashed) periods at The Bilt: numerical simulation (circles) and theoretical equation (solid and dashed lines) results.

### *D. Experimental results*

At Politecnico di Torino, a small–scale KE–yoyo prototype has been built (see Fig. 14), equipped with two Siemens® permanent-magnet synchronous motors/generators with 20–kW peak power and 10–kW rated power each. The energy produced is accumulated in a series of batteries that have a total voltage of about 340 V. The batteries also supply the energy to roll back the lines when needed. The prototype is capable of driving the flight of 5–20–m$^2$ kites with cables up to 1000 m long (see [13] for further details on the prototype). The results of the first experimental tests performed in the project are now presented and compared with numerical simulation results. In the test settings, a human operator commanded the electric drives in order to issue a desired length difference $\Delta l$ between the airfoil lines (i.e. a desired command angle $\psi$, see equation (13)) and a desired torque of the electric mo-

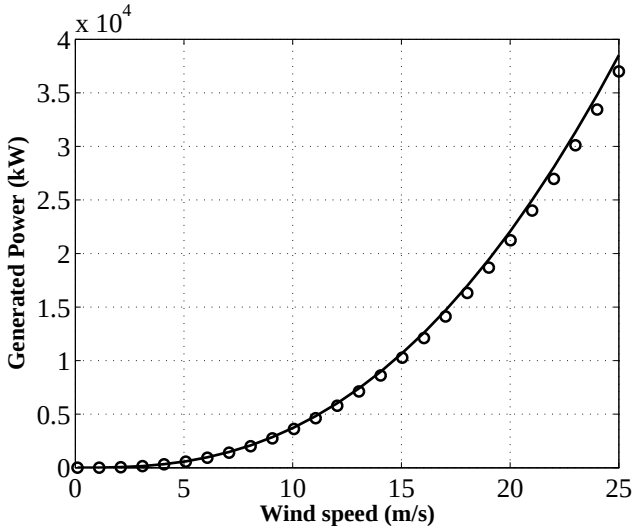


Fig. 13. Obtained net power as a function of wind speed: numerical simulation (circles) and theoretical equation (solid line) results.

tors/generators. The line length and speed have been measured through encoders placed on the electric drives. Moreover, the traction force acting on each of the lines has been measured through load cells suitably placed on the KSU. This way, by indicating with $F_1^{\mathrm{c,m}}, F_2^{\mathrm{c,m}}$ the measured traction forces of the two lines and by $\dot{r}_1^{\mathrm{m}}, \dot{r}_2^{\mathrm{m}}$ their respective rolling/unrolling speeds, the obtained mechanical power has been measured as

$$P^{\mathrm{m}} = F_1^{\mathrm{c,m}}\,\dot{r}_1^{\mathrm{m}} + F_2^{\mathrm{c,m}}\,\dot{r}_2^{\mathrm{m}}$$

The measured values of $P^{\mathrm{m}}$, sampled at a frequency of 10 Hz, have been compared with the results of numerical simulations performed with the model (18). In order to perform such numerical simulations, the initial position and velocity of the kite have been estimated on the basis of the measured line length and speed and of the line direction at the beginning of the experiment. The course of the input angle $\psi(t)$ for the simulation has been computed from the measured values of $\Delta l(t)$, using equation (13) where the distance $d$ between the attach points of the lines has been measured on the real kite. The reference line speed $\dot{r}_{\mathrm{ref}}(t)$ has been chosen as $\dot{r}_{\mathrm{ref}}(t) = (\dot{r}_1^{\mathrm{m}}(t) + \dot{r}_2^{\mathrm{m}}(t))/2$. Finally, the nominal wind speed magnitude and direction, considered for the simulations, have been estimated on the basis of a wind shear model. The latter has been identified using wind speed data collected at 3 m and at 10 m above the ground during the experiment. Indeed, the objective of these first tests of the Kitenergy technology was to test the concept and to assess the matching between real–world data and simulation results regarding the generated energy. The considered tests were performed in Sardegna, Italy, and near Torino, Italy. In the first case, the employed kite had an effective area of 5 $\mathrm{m}^2$ and the maximum line length was 300 m. A quite turbulent wind of about 4–5 m/s at ground level was present. In the second case, the employed kite had an effective area of 10 $\mathrm{m}^2$ and line length of 800 m, while the wind flow was quite weak (1–2 m/s at ground level and about 3–4 m/s at 500 m of height). Movies of the experimental tests are available [21], [22]. Fig. 15 shows the comparison between the

Fig. 14. KE–yoyo small scale prototype operating near Torino, Italy.

energy values obtained during the experimental tests and the numerical simulation results. It can be noted that quite a good matching exists between the experimental and the numerical results. The main source of error between the simulated and measured energy courses is the turbulence of wind speed (whose value at the kite's elevation could not be measured with the available test equipments), which may give rise to noticeably different instantaneous real power values with respect to the simulated ones. However, the average power values are quite similar: mean measured power values of 441 W and 555 W have been obtained in the two tests, while the simulated average values are 400 W and 510 W respectively, i.e. an error of about 10% is observed. The obtained quite good matching between the measured and simulated generated energy gives a good confidence level in the numerical and theoretical tools, which can be therefore employed to perform a realistic study of the energy generation potential of large KE–farms, composed of several KE–yoyo generators.

## IV. Capacity factor analysis

As recalled in the introduction, due to wind intermittency the average power produced by a wind generator over the year is only a fraction, often indicated as "capacity factor" (CF), of the rated power. For a given wind generator on a specific site, the CF can be evaluated knowing the probability density distribution function of wind speed and the generator wind–power curve. For example, in Table II the CFs of a KE–yoyo and of a wind tower with the power curves of Fig. 8 are

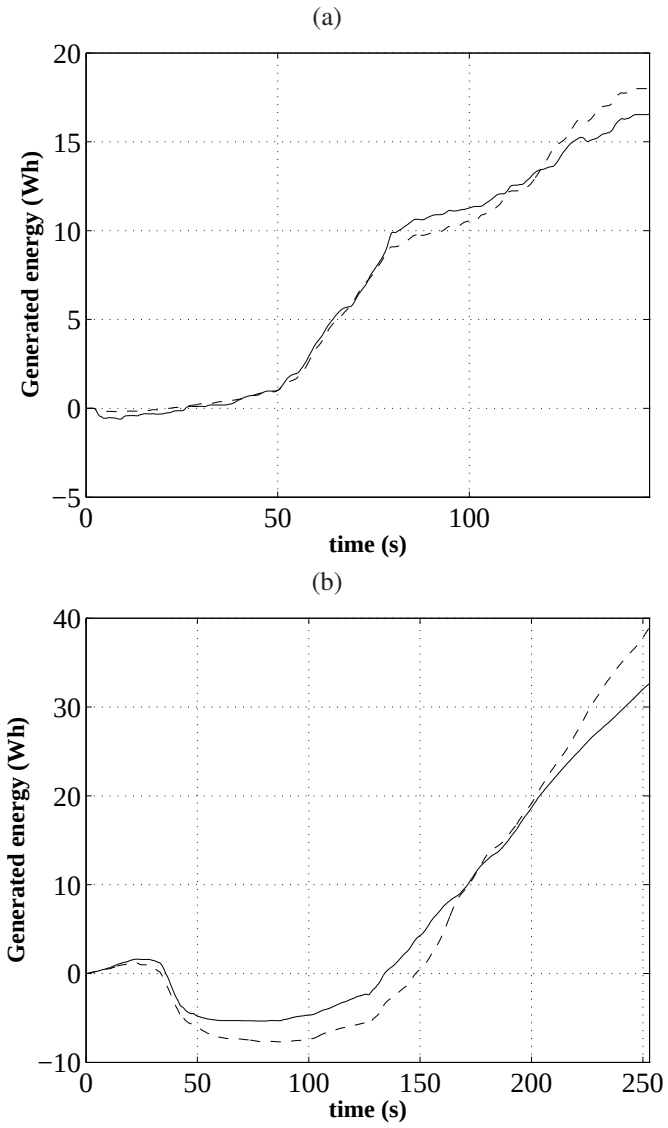


Fig. 15. Comparison between the measured (dashed) and simulated (solid) generated energy obtained with a small–scale KE–yoyo generator. The experimental tests have been carried out (a) in Sardegna, Italy, in September 2006, and (b) near Torino, Italy, in January 2008.

reported, considering some Italian sites and one location in The Netherlands. Fig. 16 shows, for two of the considered

TABLE II
CAPACITY FACTORS OF 2–MW RATED POWER WIND TOWER AND KE–YOYO AT DE BILT, IN THE NETHERLANDS, AND AT LINATE, BRINDISI AND CAGLIARI, IN ITALY, EVALUATED FROM DAILY WIND MEASUREMENTS OF SOUNDING STATIONS.

| | De Bilt | Linate | Brindisi | Cagliari |
|---|---|---|---|---|
| wind tower | 0.36 | 0.006 | 0.31 | 0.31 |
| KE–yoyo | 0.71 | 0.33 | 0.60 | 0.56 |

sites, the histograms of wind speed at 50–150 m over the ground, where the wind tower operates, and at 200–800 m over the ground, where the KE–yoyo can operate. Such estimates have been computed using the daily measurements of sounding stations collected over 11 years (between 1996 and 2006) and available on [14]. It can be noted that in all the considered sites the wind speed values between 200 m and 800 m are significantly higher than those observed between 50 m and 150 m. Considering as an example the results obtained for De Bilt (Fig. 16(a)), in the Netherlands, it can be noted that in the elevation range 200–800 m the average wind speed is 10 m/s and wind speeds higher than 12 m/s can be found with a probability of 38%, while between 50 and 150 meters above the ground the average wind speed is 7.9 m/s and speed values higher than 12 m/s occur only in the 8% of all the measurements. Similar results have been obtained with the data collected in other sites around the world. The same analysis on the data collected at Linate, Italy, leads to even more interesting results (Fig. 16(b)): in this case, between 50 and 150 meters above the ground the average wind speed is 0.7 m/s and speeds higher than 12 m/s practically never occur. On the other hand, in the operating elevation range of Kitenergy an average speed of 6.9 m/s is obtained, with a probability of 7% to measure wind speed higher than 12 m/s.

Interesting economical considerations can be drawn from the results of Table II. Note that the present wind technology is economically convenient for sites with CF $> 0.3$, according to the level of the incentives for green energy generation. In such good sites, the Kitenergy technology has capacity factors about two times greater than the present wind power technology, thus more than doubling the economic return even assuming the same costs. Indeed, for the structural reasons previously discussed, it is expected that the cost per MW of rated power of a KE–yoyo may be lower than that of a wind tower. In addition, bad sites for the present wind technology can be still economically convenient with Kitenergy technology: this is made extremely evident from the data of Linate, where a negligible CF value could be obtained with a wind tower, while a KE–yoyo could give a CF greater than that of a wind tower in the good sites of Brindisi and Cagliari.

## V. DESIGN OF LARGE SCALE KITENERGY PLANTS

The problem of suitably allocating several KE–yoyo generators on a given territory is now considered, in order to maximize the generated power per km$^2$ while avoiding collision and aerodynamic interferences among the various kites. Indeed, in the present wind farms, in order to limit the aerodynamic interferences between wind towers of a given diameter $D$, a distance of $7D$ in the prevalent wind direction and of $4D$ in the orthogonal one are typically used [5], [6].

In a KE–farm, collision and aerodynamic interference avoidance are obtained if the space regions, in which the different kites fly, are kept separated. At the same time, to maximize the generated power density per unit area of the KE–farm, it is important to keep the distance between the KSUs as short as possible. A group of 4 KE–yoyo units, placed at the vertices of a square with sides of length $L$, is now considered (see Fig. 17). The minimum cable length of the upwind kites is indicated with $\underline{r}_1$, while $\underline{r}_2$ is the minimum cable length of the downwind kites and $\Delta r$ is the cable length variation of all the kites during the flight (i.e. the maximum line lengths are $\bar{r}_1 = \underline{r}_1 + \Delta r$ and $\bar{r}_2 = \underline{r}_2 + \Delta r$). Finally, $\theta_1$ and $\theta_2$ are the average inclinations of the upwind and downwind kites respectively, with respect to the vertical axis $Z$ (see Fig. 17).

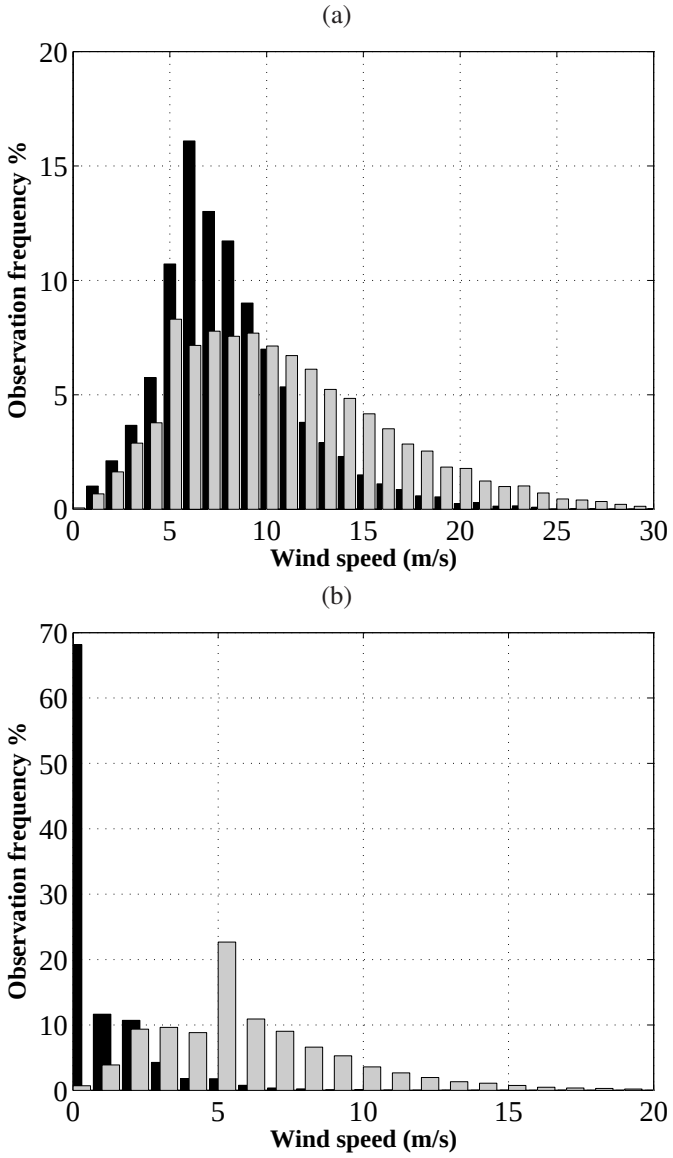


Fig. 16. Histograms of wind speed between 50 and 150 meters above the ground (black) and between 200 and 800 meters above the ground (gray). Data collected at (a) De Bilt (NL) and (b) Linate (IT).

For given characteristic of wind, kite, cables, etc., the values of $\theta_1, \underline{r}_1, \theta_2, \underline{r}_2, \Delta r$, and $L$ can be computed to maximize the average net power per unit area generated by the four KE–yoyo generators, subject to the constraints that the polyhedra limiting the kite flight regions do not intersect and that the maximum flight elevation of the downwind kites is lower than the minimum elevation of the upwind ones, so to avoid aerodynamic interferences. In particular, denote with $\overline{P}_1$ and $\overline{P}_2$ the average power obtained by the upwind and by the downwind generators respectively. As shown in Section III-B (equation (20)), $\overline{P}_1$ and $\overline{P}_2$ are functions of $\theta_1, \underline{r}_1, \theta_2, \underline{r}_2, \Delta r$ and of the line unrolling speed values $\dot{r}_1^{\text{trac}}$ and $\dot{r}_2^{\text{trac}}$ of the upwind and downwind KE–yoyo respectively. Note that a value of $\phi = 0$ (i.e. the cables are aligned with the nominal wind speed direction in the $(X, Y)$ plane) is considered for the computation of $\overline{P}_1, \overline{P}_2$ in (20), since it gives the maximal power with respect to any other $\phi$ value. It can be shown that the power density $\overline{P}_D$ per unit area is given by:

$$\overline{P}_D = \frac{(\overline{P}_1 + \overline{P}_2)}{2} \frac{1}{L^2} \tag{23}$$

Thus, the power density of the considered group of KE–yoyo units is given by the mean power of two subsequent units (along the wind direction) divided by the square of their distance. The value of $\overline{P}_D$ (23) clearly depends on the involved operational and design parameters. Thus, the following numerical optimization problem can be set up and solved to design the KE–farm configuration and operation:

$$\begin{gathered}
(\theta_1^*, \underline{r}_1^*, \dot{r}_1^{\text{trac}*}, \theta_2^*, \underline{r}_2^*, \dot{r}_2^{\text{trac}*}, \Delta r^*, L^*) = \arg\max \overline{P}_D \\
\text{subject to} \\
\underline{Z} - \underline{r}_1 \cos(\theta_1 + \Delta\theta_1) \leq 0 \\
\underline{Z} - \underline{r}_2 \cos(\theta_2 + \Delta\theta_2) \leq 0 \\
F_1^{\text{c,trc}} - 2c_s \overline{F}(d_l) \leq 0 \\
F_2^{\text{c,trc}} - 2c_s \overline{F}(d_l) \leq 0 \\
(\underline{r}_2 + \Delta r)\cos(\theta_2 - \Delta\theta_2) - \underline{r}_1 \cos(\theta_1 + \Delta\theta_1) \leq 0 \\
\underline{r}_1 \sin(\Delta\theta_1) - \frac{L}{2} \leq 0 \\
\underline{r}_2 \sin(\Delta\theta_2) - \frac{L}{2} \leq 0 \\
((\underline{r}_2 + \Delta r)\sin(\theta_2 + \Delta\theta_2) - L)/\tan(\theta_1 - \Delta\theta_1) \\
-(\underline{r}_2 + \Delta r)\cos(\theta_2 + \Delta\theta_2) \leq 0 \\
(\underline{r}_2 + \Delta r)\cos(\theta_2 - \Delta\theta_2) \\
-(L + (\underline{r}_2 + \Delta r)\sin(\theta_2 - \Delta\theta_2))/\tan(\theta_1 + \Delta\theta_1) \leq 0 \\
\Delta\theta_1 - \theta_1 \leq 0 \\
\Delta\theta_2 - \theta_2 \leq 0
\end{gathered} \tag{24}$$

where $\Delta\theta_1 = \frac{a}{2(\underline{r}_1)}$ and $\Delta\theta_2 = \frac{a}{2(\underline{r}_2)}$ and $a$ is the side of the polyhedral zone in which the kite trajectory is kept (see Fig. 3). $F_1^{\text{c,trc}}$ and $F_2^{\text{c,trc}}$ are the traction forces exerted by the upwind and downwind kites (computed as in (22)), while function $\overline{F}(d_l)$ gives the minimal breaking load of each cable (according to the curve reported in Fig. 9) and $c_s$ is a safety coefficient. The constraints included in (24) prevent interference between the airfoil flying zones, both in the parallel and perpendicular directions with respect to the wind, avoid excessive traction forces and impose a minimal flying height equal to $\underline{Z}$. Using the system data given in Table I, with $\underline{Z}$=30 m, $c_s$=2 and $a$=300 m and the wind shear profile $W_x(Z)$ corresponding to summer months at the Bilt (reported in Fig. 5), the solution of the optimization problem (24) is $\theta_1^* = 46.5^\circ$, $\dot{r}_1^{\text{trac}*} = 2.3$ m/s, $\underline{r}_1^* = 1100$ m, $\theta_2^* = 51.7^\circ$, $\dot{r}_2^{\text{trac}*} = 2.2$ m/s, $\underline{r}_2^* = 530$ m, $\Delta r^* = 50$ m and $L^* = 250$ m. With such a solution, the kite flight elevations are between about 650 m and 850 m for the upwind kites and between about 350 m and 550 m for the downwind kites. Similar values are obtained also for the other sites considered in Table II. Then, several of such groups of 4 KE–yoyo generators can be placed at a distance of $L^* = 250$ m one from the other, so to avoid collisions among kites of adjacent basic units. With this solution, the kites flying at the same elevation, belonging to adjacent basic units in line with the wind, result to be at a distance of 500 meters, with limited expected aerodynamic interferences. This way, it is possible to realize KE–farms with a density of 16 KE–yoyo units per km$^2$ and, consequently, a rated power of 32 MW per km$^2$, with a capacity factor of about 0.6 in a good site like De Bilt in the Netherlands. Indeed, as previously noted, the same 500–m$^2$ kite can be used to obtain a KE–yoyo with 5

MW rated power, without significant cost increases, except for the electric equipments. Then, a KE–farm using such 5–MW KE–yoyo would have a rated power density of 80 MW per km$^2$ and a capacity factor of about 0.45 in a site like De Bilt. Note that a wind farm realized with 2–MW, 90–m diameter wind towers has a density of 4.5 towers per km$^2$ and a rated power of about 9 MW per km$^2$ [3], [6], with a capacity factor of about 0.3–0.4 in a good site.

Thus, the presented analysis shows that a suitably designed KE–farm could provide a rated power per unit area from 3.5 to 9 times higher than that of a present wind tower farm, for the 2–MW and 5–MW KE–yoyo respectively, with a consequent average yearly generated power per km$^2$ ranging from 7 to 13 times the value obtained by wind towers.

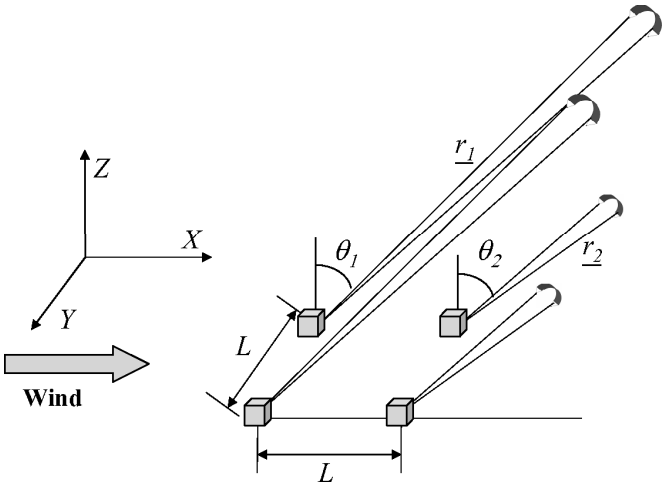


Fig. 17. Group of 4 KE–yoyo placed on the vertices of a square land area.

## VI. Energy production costs of Kitenergy

On the basis of the results presented so far, a preliminary estimate of the costs of the electricity produced with Kitenergy can be performed to make a comparison with the costs of the other technologies. The production costs for Kitenergy and wind tower technologies are related essentially to the amortization of the costs of the structures, the foundations, the electrical equipments to connect to the power grid, authorizations, site use, etc., while the maintenance costs are certainly marginal for both technologies, though possibly higher for Kitenergy. Thus, the main differences between the two technologies are related to their structures, foundations and required land, whose costs are significantly lower for Kitenergy. In fact, the heavy tower and the rotor of a wind turbine are replaced by light composite fiber cables and the kite in a KE–yoyo. Given the same rated power, the foundations of a KE–yoyo have to resist to significantly lower strains. A reliable estimate of the energy production costs of a KE–farm certainly requires more experimentations. However, for all the aspects discussed so far, a very conservative estimate can be obtained, at least in relative terms with respect to the cost of the actual wind technology, by assuming that the cost of a KE–yoyo unit with 2–MW rated power is not greater than that of an actual wind tower with 2–MW rated power.

Table III shows the projected cost in 2030 (levelised in 2003 U.S. dollars per MWh) of energy from coal, gas, nuclear, wind and solar sources. The costs reported in Table III have been taken from [23] where, for each technology, the projections have been computed using data related to power plants installed in more than 10 different countries. Such data, provided by experts from the participating countries, include cost data and technical information. In particular, an average load factor of 85% for coal, gas and nuclear power plants has been considered, as well as a capacity factor from 17% to 38% for wind power and an availability/capacity factor from 9% to 24% for solar plants. Moreover, economic lifetime of 40 years and discount rate of 5% have been taken into account, while the costs associated with residual emission (including greenhouse gases) have not been considered (for more details on the methodology employed to estimate the energy costs of Table III, the interested reader is referred to [23]). The average estimated costs reported in Table III have been computed considering, for each source, all of the power plants analyzed in [23].

TABLE III
Projected cost in 2030 (levelised in 2003 U.S. dollars per MWh) of energy from different sources, compared with the estimated energy cost of Kitenergy.

| Source | Minimal estimated ($/MWh) | Maximal estimated ($/MWh) | Average estimated ($/MWh) |
|---|---|---|---|
| Coal | 25 | 50 | 34 |
| Gas | 37 | 60 | 47 |
| Nuclear | 21 | 31 | 29 |
| Wind | 35 | 95 | 57 |
| Solar | 180 | 500 | 325 |
| Kitenergy | 10 | 48 | 20 |

According to [23], considering sites with CF between 17% and 38%, the projected energy production costs of a wind farm composed of 2–MW towers is between 35 $/MWh and 95 $/MWh with a density of about 4.5 towers per km$^2$ (assuming a diameter $D$ =90 and applying the "7$D$–4$D$ rule" [3], [6]). On the basis of the analyses presented in this paper, in the same location a KE–farm of the same overall rated power, composed of 2–MW KE–yoyo units using 500–m$^2$ kites, would produce an average power 2 times higher than that of the wind farm (thanks to the greater capacity factor), with a density of 16 KE–yoyo per km$^2$, i.e. 3.6 times higher than the wind farm. Then, a conservative energy cost estimate between 18 $/MWh and 48 $/MWh is obtained for Kitenergy. Note that the considered cost assumption is a very conservative one and that the higher density of KE–yoyo units leads to lower land occupation (i.e. lower costs) for the same rated power. Moreover, the study presented in Section V shows that with the only additional costs related to the replacement of the 2–MW electric systems with 5–MW ones, the same KE–farm, i.e. with the same 500–m$^2$ kites, can reach a rated power 2.5 times higher and an average yearly power 3.75 times higher than those of the wind tower farm. Note that, in order to increase the rated and average generated power of an actual wind farm, much higher investments would be needed, since higher

and bulkier towers with bigger rotors should be employed to obtain adequate CF values. Thus, scale factors positively affect the production costs of Kitenergy technology, leading to cost estimates (reported in Table III) of 10–48 $/MWh with an average value of 20 $/MWh, showing that high–altitude wind energy may be significantly cheaper than fossil energy.

## VII. Conclusions

The paper described the advances of the Kitenergy project, including numerical simulations and prototype experiments. Wind data analyses, a study on the design of large kite power plants and a preliminary electricity cost analysis have been also presented, showing that the Kitenergy technology, capturing the wind power at significantly higher altitude over the ground than the actual wind towers, has the potential of generating renewable energy, available in large quantities almost everywhere, with production cost lower than that of fossil energy.

Thus, high–altitude wind power may contribute to a significant reduction of the global dependance on the fossil sources in a relatively short time. Indeed, the industrialization of this technology may require from 3 to 5 years, since no breakthrough is actually needed in any of the involved engineering fields (like aerodynamics and flight mechanics, materials, modeling and control theory, mechatronics,etc.) to apply this technology, but rather the fusion of advanced competencies, already existing in each field, in order to increase the efficiency and the reliability of the system. Indeed, substantial new technological innovations, for example in the field of high–efficiency airfoils, may lead to further great performance improvements.

## References


[1] International Energy Agency (IEA), *World Energy Outlook 2008*. Paris, France: IEA PUBLICATIONS, 2008.

[2] "Global Wind Energy Council, *Global wind 2007 report*," May 2008, (Available online: http://www.gwec.net/fileadmin/documents/test2/gwec-08-update_FINAL.pdf).

[3] C. L. Archer and M. Z. Jacobson, "Evaluation of global wind power," *J. Geophys. Res.*, vol. 110, D12110, 2005.

[4] R. Thresher, M. Robinson, and P. Veers, "To capture the wind," *IEEE Power & Energy Magazine*, vol. 5, no. 6, pp. 34–46, 2007.

[5] M. Z. Jacobson and G. M. Masters, "Exploiting wind versus coal," *Science*, vol. 293, p. 1438, 2001.

[6] G. M. Masters, *Renewable and Efficient Electric Power Systems*. Wiley, 2004.

[7] M. L. Loyd, "Crosswind kite power," *Journal of Energy*, vol. 4, no. 3, pp. 106–111, 1980.

[8] M. Canale, L. Fagiano, and M. Milanese, "Power kites for wind energy generation," *IEEE Conrol Systems Magazine*, vol. 27, no. 6, pp. 25–38, 2007.

[9] B. Houska, "Robustness and stability optimization of open-loop controlled power generating kites," Master's thesis, University of Heidelberg, 2007.

[10] B. W. Roberts, D. H. Shepard, K. Caldeira, M. E. Cannon, D. G. Eccles, A. J. Grenier, and J. F. Freidin, "Harnessing high–altitude wind power," *IEEE Transactions on Energy Conversion*, vol. 22, no. 1, pp. 136–144, 2007.

[11] Vestas Wind Systems A/S website, 2009: http://www.vestas.com.

[12] M. Canale, L. Fagiano, and M. Milanese, "High altitude wind energy generation using controlled power kites," *IEEE Transactions on Control Systems Technology*, available on-line, 2009. doi: 10.1109/TCST.2009.2017933

[13] L. Fagiano, "Control of tethered airfoils for high–altitude wind energy generation," Ph.D. dissertation, Politecnico di Torino, Italy, February 2009, available on–line: http://lorenzofagiano.altervista.org/docs/PhD_thesis_Fagiano_Final.pdf.

[14] NOAA/ESRL Radiosonde Database Access, 2009: http://raob.fsl.noaa.gov/.

[15] M. Diehl, "Real-time optimization for large scale nonlinear processes," Ph.D. dissertation, University of Heidelberg, Germany, 2001.

[16] G. M. Maneia, "Aerodynamic study of airfoils and wings for power kites applications," Master's thesis, Politecnico di Torino, October 2007, available on–line: http://lorenzofagiano.altervista.org/docs/MasterThesisManeia.rar.

[17] B. Houska and M. Diehl, "Optimal control for power generating kites," in *9th European Control Conference*, Kos, GR, 2007, pp. 3560–3567.

[18] F. Allgöwer and A. Zheng, *Nonlinear model predictive control*. New York: Wiley, 2000.

[19] M. Canale, L. Fagiano, and M. Milanese, "Fast nonlinear model predictive control using Set Membership approximation," in *17th IFAC World Congress*, Seoul, Korea, 2008, pp. 12 165–12 170.

[20] ——, "Set Membership approximation theory for fast implementation of model predictive control laws," *Automatica*, vol. 45, no. 1, pp. 45–54, 2009.

[21] Kitenergy project, experimental test movie, (2008, Jan.), [Online]. Available: http://lorenzofagiano.altervista.org/movies/Casale_test.wmv

[22] Kitenergy project, experimental test movie (2006, Aug.), [Online]. Available: http://lorenzofagiano.altervista.org/movies/Sardinia_test.wmv

[23] International Energy Agency (IEA), *Projected Cost of Generating Energy – 2005 update*. Paris, France: IEA PUBLICATIONS, 2008, available on–line: http://www.iea.org/Textbase/publications/free_new_Desc.asp?PUBS_ID=1472.


**Lorenzo Fagiano** (M'07) received the Bachelor's degree in automotive engineering in 2002, the Master's degree in automotive engineering in 2004 and the Ph.D. degree in information and system engineering in 2009 from Politecnico di Torino, Italy. In 2005 he worked for Fiat Research Centre, Italy, in the active vehicle systems area. Currently he holds a post-doctoral position at Politecnico di Torino, Italy. His main research interests include constrained robust and nonlinear control and set membership theory for control purposes, applied to automotive control and high–altitude wind energy generation.

**Mario Milanese** (M'90–SM'04) graduated in electronic engineering at Politecnico di Torino, Torino, Italy, in 1967. Since 1980, he has been a full professor of system theory at Politecnico di Torino. From 1982 to 1987, he was head of the Dipartimento di Automatica e Informatica at the Politecnico di Torino. His research interests include identification, prediction, and control of uncertain systems with applications to biomedical, automotive, aerospace, financial, environmental, and energy problems. He is the author of more than 200 papers in international journals and conference proceedings.

**Dario Piga** (M'09) received the Bachelor's degree in electronics engineering in 2004 and the Master's degree in mechatronics/robotics engineering in 2008 both at the Politecnico di Torino. From April 2008 to December 2008 he worked as assistant researcher at the Dipartimento di Automatica ed Informatica of the Politecnico di Torino. Since January 2009 he has been a Ph.D. student at the same department. His main research interests include set membership identification of block-oriented models, optimal robust control and filtering and analysis and control of Kitenergy system.